doi:10.1016/j.jmb.2010.01.060 J. Mol. Biol. (2010) 397, 1339–1349

JMB

Available online at www.sciencedirect.com

ScienceDirect

ELSEVIER

A Conserved Protonation-Induced Switch can Trigger "Ionic-Lock" Formation in Adrenergic Receptors

Stefano Vanni, Marilisa Neri, Ivano Tavernelli and Ursula Rothlisberger*

Laboratory of Computational Chemistry and Biochemistry, Ecole Polytechnique Fédérale de Lausanne, CH-1015 Lausanne, Switzerland

Received 16 November 2009; received in revised form 19 January 2010; accepted 25 January 2010
Available online
2 February 2010

The mechanism of signal transduction in G-protein-coupled receptors (GPCRs) is a crucial step in cell signaling. However, the molecular details of this process are still largely undetermined. Carrying out submicrosecond molecular dynamics simulations of β-adrenergic receptors, we found that cooperation between a number of highly conserved residues is crucial to alter the equilibrium between the active state and the inactive state of diffusible ligand GPCRs. In particular, "ionic-lock" formation in β-adrenergic receptors is directly correlated with the protonation state of a highly conserved aspartic acid residue [Asp(2.50)] even though the two sites are located more than 20 Å away from each other. Internal polar residues, acting as local microswitches, cooperate to propagate the signal from Asp(2.50) to the G-protein interaction site at the helix III–helix VI interface. Evolutionarily conserved differences between opsin and non-opsin GPCRs in the surrounding of Asp(2.50) influence the acidity of this residue and can thus help in rationalizing the differences in constitutive activity of class A GPCRs.

Keywords: GPCR; signal transduction; molecular dynamics; adrenergic receptor

Edited by D. Case

Introduction

G-protein-coupled receptors (GPCRs) are a large family of integral membrane proteins involved in many pathways responsible for signal transduction into the cell, and they nowadays constitute the largest class of drug targets.[1] Despite intense research efforts during the last decades that have led to wide characterization of GPCRs in terms of function and ligand-binding properties, structure determination has been quite elusive, and only recently were Cherezov *et al.*[2] and Warne *et al.*[3] able to resolve the crystal structures of two of the most studied GPCRs able to bind diffusible ligands: β_2-adrenergic receptor (β_2AR) and β_1AR.

The common framework to describe receptor activation supports the coexistence of several conformational intermediates and the occurrence of biased agonism, suggesting equilibrium between active and inactive states.[4] While it is widely acknowledged that GPCR function relies on the ability to adopt multiple conformations to activate/inhibit the signaling cascade, the lack of extensive structural data implies that the atomistic details of the multistep process leading to GPCR activation are still unclear.

Several experiments identified some conserved regions in GPCRs that upon mutations could lead to a shift in this equilibrium.[5–16] Among them, disruption of the salt bridge ("ionic lock") between Arg (3.50) of the (D/E)RY motif of helix III and a partially conserved Glu(6.30) of helix VI seems to be a crucial feature of the early steps of receptor activation.[5,7,8] This conformational fingerprint is present in all the crystal structures of inactive rhodopsin,[17–19] and, despite being absent in the crystal structures of engineered β-adrenergic receptors, it has independently been observed in different microsecond molecular dynamics (MD) simulations of reconstructed wild-type adrenergic receptors bound to inverse agonists.[20,21] The recently solved crystal structure of ligand-free opsin in its "active-like" conformation[22] has provided a high-resolution description of an activated receptor. In agreement with site-directed spin-labeling experiments[23] and double electron–electron resonance spectroscopy,[24] outward movement of the intracellular part of helix VI (that tilts outward by 6–7 Å with respect to the

*Corresponding author. E-mail address: ursula.roethlisberger@epfl.ch.

Abbreviations used: GPCR, G-protein-coupled receptor; $\beta_{1/2}$AR, $\beta_{1/2}$-adrenergic receptor; MD, molecular dynamics.

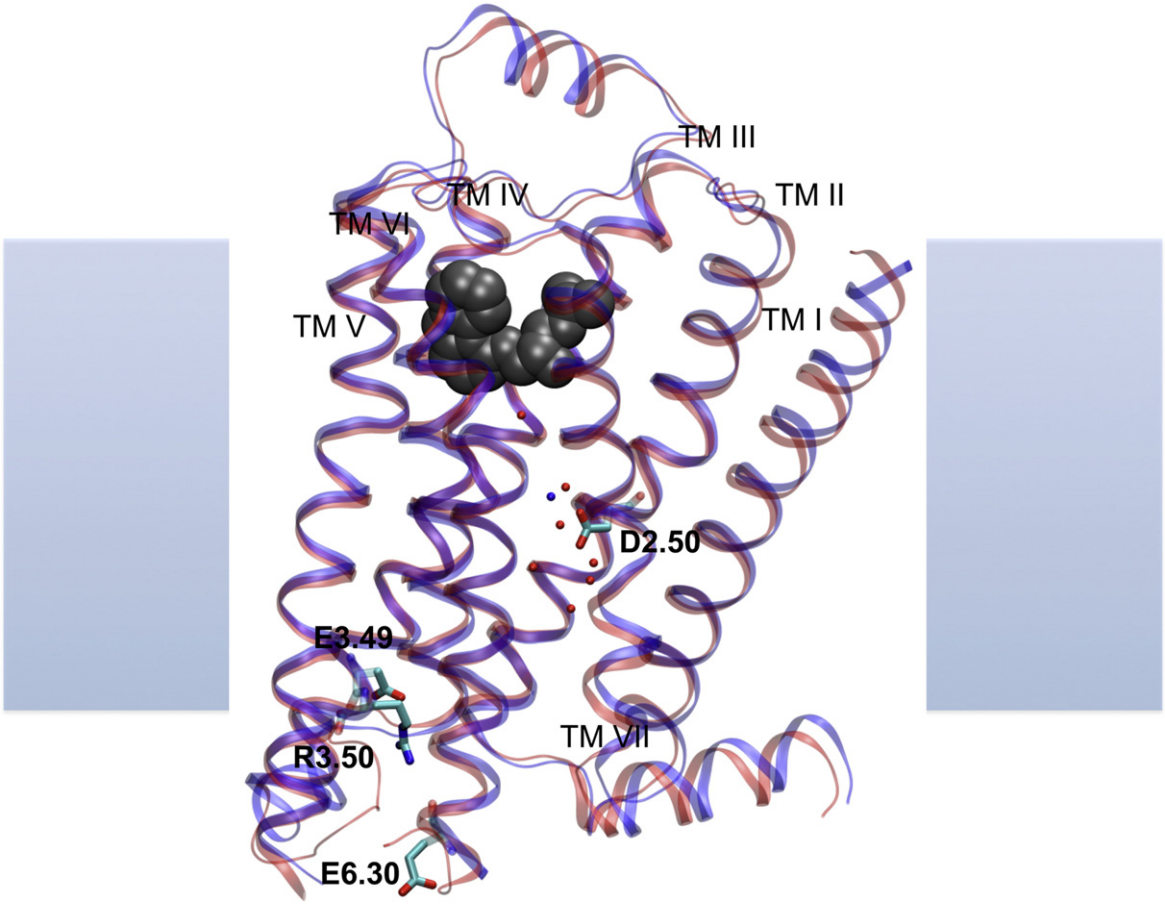

Fig. 1. Localization of the bound ligand (shown in gray in space-filling representation) and of crucial titrable residues Asp(2.50), Glu(3.49), Arg(3.50) and Glu(6.30) in the crystal structures of β_1AR (backbone represented in blue) and β_2AR (backbone represented in red). Crystallographic water molecules within 5 Å of Asp(2.50) are shown in red for β_2AR and in blue for β_1AR.

structure of dark-state rhodopsin) is required for activation. This movement is associated with a conformational change of Arg(3.50) of the ionic lock that adopts an extended conformation pointing toward the protein core that enables direct interaction with the G-protein fragment.

Even though biochemical experiments suggest that the global structural features of active and inactive states of GPCRs are very similar across the entire family,[25] almost all GPCRs, apart from the opsin family that binds ligands covalently, are able to reversibly bind a large number of diffusible ligands. Interestingly, diffusible ligand GPCRs show a considerable amount of basal, agonist-independent activity, while rhodopsin has almost no detectable basal activity in the absence of light, suitable for its biological function as a highly sensitive pigment.[26] The ability of the receptor to activate a given signaling pathway is substantially altered upon ligand binding, and recent findings based on fluorescence resonance energy transfer experiments suggest that different ligands can trigger independent functional states, thus stabilizing the cytoplasmic moiety of the receptor in a given signaling conformation.[27–29]

At the same time, while the global mechanism of receptor activation is quite established, the way the receptors perform signal transduction upon ligand recognition from the binding pocket into the cytoplasmic moiety is not yet understood. Mutational studies have indicated that some residues are essential for receptor function, and it has also been proposed that the presence of a number of conserved water molecules in the hydrophobic interhelical core of GPCRs could play a significant role.[12,13,16,30,31] Interestingly, there is only one titrable residue in the highly hydrophobic core of adrenergic receptors (Fig. 1), as well as in rhodopsin†, the widely conserved Asp(2.50). Mutational studies on a large number of GPCRs have indicated that mutation of this residue leads to reduced or abolished ability of the receptor to activate its partner G-protein[12,13,32,33] and to altered constitutive activity[34] in diffusible ligand GPCRs or to a forward shift in the MetaI–MetaII equilibrium in rhodopsin.[35] In the case of rhodopsin, spectroscopic experiments have determined that this residue is protonated in both the dark state and in the activated

† Residue Glu(3.41) in adrenergic receptors and residues Glu(3.37) and His(5.46) in rhodopsin are located within the transmembrane region but are pointing toward the lipid environment, not toward the interhelical core of the receptors.

(MetaII) form and that it changes hydrogen-bond partners upon activation.[36,37] On the other hand, Asp (2.50) has been identified as an ion-responsive motif for a large number of diffusible ligand class A GPCRs, including adrenergic receptors, and several experiments support cationic regulation of signal transduction in such GPCRs,[33,38] suggesting that Asp (2.50) can bear a negative charge in these systems.

To understand the possible role of Asp(2.50) in GPCR signal transduction, we performed microsecond MD simulations of β_1AR and of β_2AR for both possible protonation states of Asp(2.50). Anticipating our results, we found a strong correlation between the protonation state of Asp(2.50) and formation or breaking of the ionic lock, thus indicating that the protonation state of this residue has a direct role in the activation/inhibition of adrenergic receptors. Moreover, we identified a number of conserved internal polar residues that act as local microswitches and cooperate to propagate the signal directly from Asp(2.50) to the G-protein interaction site at the helix III–helix VI interface.

Results

Asp(2.50) acidity

The aspartic acid Asp(2.50) is the only titrable group inside the heptahelical core of adrenergic receptors (Fig. 1). Both its special location and degree of conservation, as well as a large number of biochemical experiments, suggest that this residue is involved in signal transduction. Identification of its protonation state is therefore crucial. Fourier transform infrared experiments have determined that Asp(2.50) is protonated in both the dark state and in the activated (MetaII) state of rhodopsin,[36,37] while it has been identified as a cation-responsive motif for a number of class A GPCRs, including adrenergic receptors, thus suggesting that the residue can be negatively charged under *in vivo* conditions.[33,38]

Despite the fact that the available X-ray data of GPCRs describe the receptors in potentially different signaling states, it is interesting to notice that the immediate surroundings of Asp(2.50) as observed in the crystal structures can vary significantly: Asp(2.50) is surrounded‡ by five water molecules in the crystal structure of β_2AR-T4L[2] and by only one water molecule (Fig. 1) in the crystal structure of β_1AR-m23,[3] while a maximum of two water molecules in the proximity of Asp(2.50) have been identified in different crystal structures of inactive rhodopsin.[17–19]

Electrostatic calculations and empirical pK_a estimates based on the crystal structures (cf., Table 1) indicate that Asp(2.50) has a pK_a in adrenergic receptors§ lower than that in inactive rhodopsin.

‡ Defined as within 5 Å from any atom of Asp(2.50).

§ In addition, due to the more hydrophobic surroundings, the pK_a of Asp(2.50) in β_1AR-m23 is slightly lower than that in β_2AR-T4L.

Table 1. Computed pK_a values of Asp(2.50) in the crystal structure of inactive rhodopsin and β-adrenergic receptors

		Poisson–Boltzmann			
GPCR	PDB ID	$\varepsilon=4$	$\varepsilon=10$	$\varepsilon=20$	PROPKA[65]
Inactive rhodopsin	1U19[18]	20.9	9.6	6.7	7.6
β_2AR-T4L	2RH1[2]	9.5	5.5	4.3	6.9
β_1AR-m23	2VT4[3]	9.9	6.2	5.0	6.2

Comparison between the crystal structures (Fig. 2) suggests that this difference originates from polar substitutions surrounding Asp(2.50) that are present in adrenergic receptors but absent in rhodopsin. In particular, Ala(3.39)→Ser(3.39) [with the side-chain hydrogen of Ser(3.39) pointing toward Asp(2.50)] and Ser(7.45)Ala(7.46)→Asn(7.45)Ser(7.46) (Fig. 2) are likely to favor a negative charge on Asp(2.50).

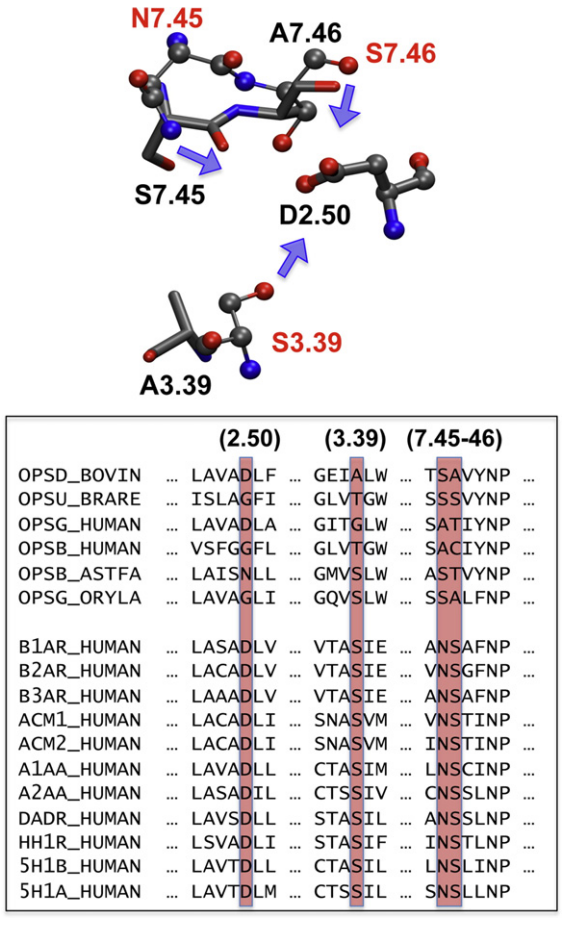

Fig. 2. Comparison of Asp(2.50) surroundings in rhodopsin and adrenergic receptors. The upper panel shows the structural alignment of positions 2.50, 3.39, 7.45 and 7.46 in the crystal structures of rhodopsin (black, licorice representation) and β_2AR (red, ball-and-stick representation). The blue arrows indicate dipole moments that constitute the polar environment that can stabilize Asp(2.50) in the deprotonated form. The lower panel shows the sequence alignment of positions 2.50, 3.39, 7.45 and 7.46 between class A GPCRs (illustrative; cf., Ref. 39).

Table 2. RMSD average values of crystallographic C^{α}, transmembrane helix backbone, binding pocket, Asp(2.50) surroundings, extracellular helix backbone and intracellular helix backbone

RMSD (Å)	Crystallographic C^{α}	Transmembrane helix backbone	Binding pocket[a]	Asp(2.50) surroundings[b]	Extracellular helix backbone	Intracellular helix backbone
β_2AR-wt-deprot	1.2	0.9	1.0	0.9	1.0	1.1
β_2AR-wt-prot	1.5	1.2	0.9	1.0	1.1	1.3
β_1AR-wt-deprot	1.9	1.6	0.9	1.4	1.2	2.1
β_1AR-wt-prot	1.5	1.1	0.9	1.0	1.0	1.2
β_1AR-m23-deprot	1.3	1.0	0.8	1.0	1.0	1.2
β_1AR-m23-prot	1.8	1.4	0.9	1.0	1.1	1.9

[a] Defined as residues within 5 Å from any atom of the ligand in the crystal structures.
[b] Defined as residues within 5 A from any atom of Asp(2.50) in the crystal structures.

Conservation analysis between class A GPCRs (based on the sequence alignment proposed by Man *et al.*[39]) shows that this hydrophobic-to-polar shift is not a peculiar property of opsins with respect to adrenergic receptors but is a general characteristic of opsin *versus* non-opsin GPCRs. In particular, if we exclude odorant receptors‖, it is remarkable that Asp (2.50) is perfectly conserved in non-opsin class A GPCRs, while this is not the case for the opsin family. Moreover, the strict conservation of a serine at position 3.39 of non-opsin receptors suggests that this residue is essential for the correct function of these receptors, while in opsins a serine is present at position 3.39 only when there is no aspartate at position 2.50. At the same time, the polar pair Asn–Ser at positions 7.45–7.46 is highly conserved in non-opsin class A GPCRs, while it is not in the opsin family. These differences between opsin and non-opsin receptors suggest that a negative charge is favored inside the heptahelical core of adrenergic receptors with respect to rhodopsin as a consequence of conserved substitutions in the surroundings that introduce charge-stabilizing dipoles.

Taken together, electrostatic calculations and conservation analysis suggest an intrinsic difference between opsin and non-opsin class A GPCRs that relates to a possibly different role of Asp(2.50) in the two families. It must be noted that opsins are peculiar among class A GPCRs both because they are the only family that binds their agonist covalently and because of the lack of constitutive activity.

Ionic-lock configuration is correlated with protonation state of Asp(2.50)

To study the possible effects of the protonation state of Asp(2.50) on receptor function, we performed MD simulations between 500 and 800 ns of β_1AR-m23, of wild-type β_1AR bound to the antagonist cyanopindolol [Protein Data Bank (PDB) entry 2VT4] and of wild-type β_2AR bound to the inverse agonist carazolol (PDB entry 2RH1) for both possible protonation states of Asp(2.50) (cf., Materials and Methods).

After equilibration of the systems in both protonation states, we observed only very low deviations from the crystal structures in all simulations (average backbone helix RMSD of all simulations, 1.2 Å), especially also for the binding pocket (average RMSD, 0.9 Å) and the surroundings of Asp(2.50) (average RMSD, 1.1 Å), suggesting that protonation/deprotonation does not induce significant local structural rearrangements (cf., Table 2). These results reinforce the possibility that the crystal structures are easily compatible with both protonation states.

However, despite the limited overall conformational changes, it is remarkable that significant deviations occur in the cytoplasmic end of the receptor (cf., Table 2), a site that is able to adopt different conformations to interact with the partner G-protein and trigger the signaling cascade.[25] In particular, main differences exist for the region of the ionic lock as demonstrated by the values of the C^{α}–C^{α} distance and of the shortest N–O distance between Arg(3.50) and Glu(6.30) (Fig. 3), the two residues located at the cytoplasmatic ends of helices III and VI that are expected to form a salt bridge (ionic lock) in the inactive form of the receptors. In particular, taking as a reference value the C^{α}–C^{α} distance between these two residues¶, it is remarkable that in all systems, protonation of Asp(2.50) leads to stabilization of the receptors in an inactive-like conformation where the ionic lock between helices III and VI is formed and the average C^{α}–C^{α} distance along the simulations is comparable with the X-ray structures of inactive rhodopsin (Fig. 3).

On the other hand, simulations of adrenergic receptors with Asp(2.50) deprotonated consistently show no formation of the ionic lock between helices III and VI (Fig. 3), except for very short time windows. In particular, the equilibrium geometry of the C^{α}–C^{α} distance between Arg(3.50) and Glu (6.30) is above the corresponding distance of inactive rhodopsin crystal structures for most of the simulation time. Interestingly, even if the salt bridge between Arg(3.50) and Glu(6.30) is occasionally formed, this interaction is unstable in all

‖ In several odorant receptors, Asp(2.50) is replaced by a glutamate, while the polar environment resembles that of adrenergic receptors.

¶ The C^{α}–C^{α} distance between Arg(3.50) and Glu(6.30) is 8.7 Å in inactive rhodopsin (PDB entry 1F88), while it is 14.7 Å in active opsin (PDB entry 3CAP).

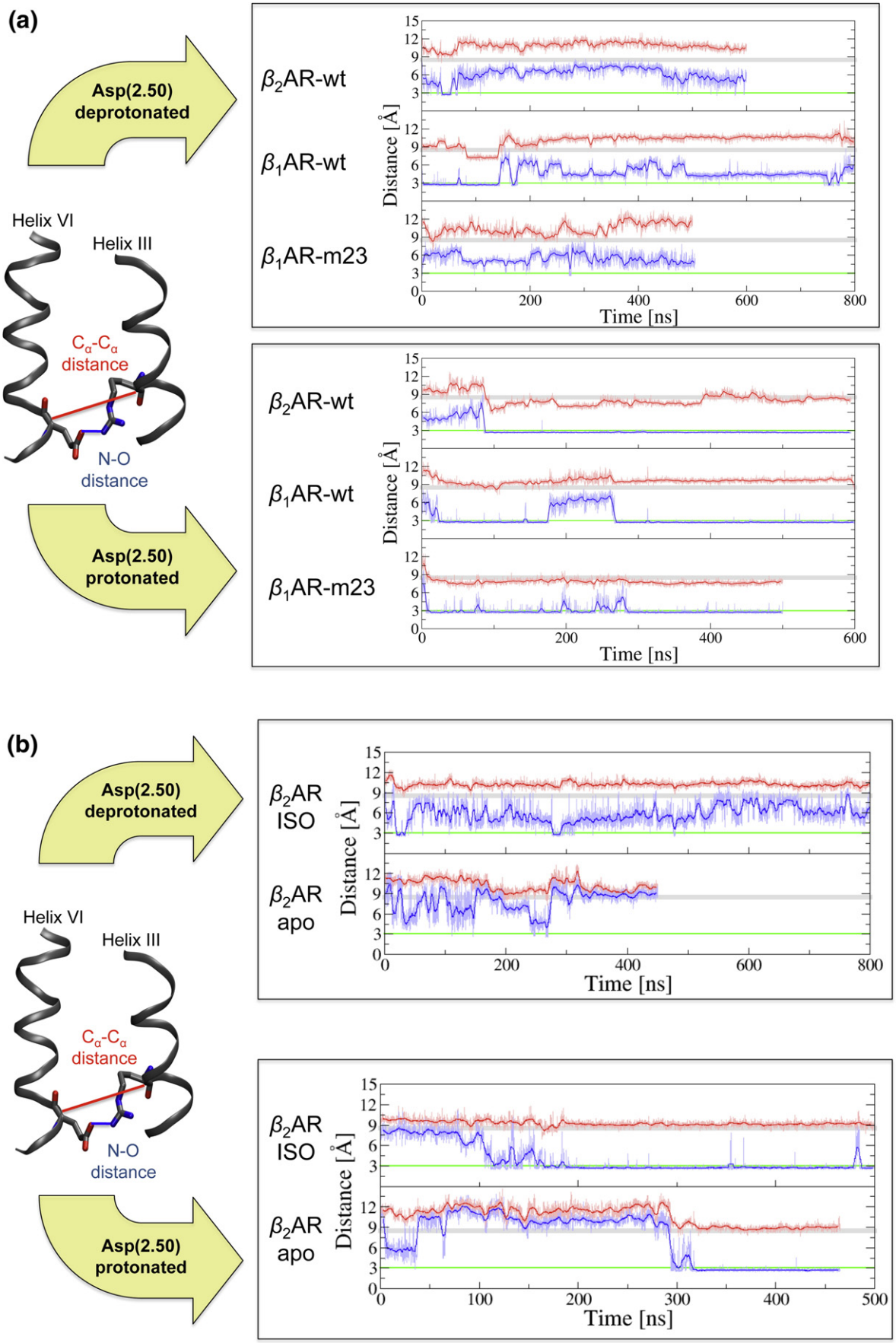

Fig. 3 (*legend on next page*)

simulations and separation between the two residues is achieved within tens of nanoseconds. On the other hand, the critical[11] intrahelical salt bridge between Arg(3.50) and Asp(3.49) remains intact in all simulations, with the exception of wild-type β_1AR with a deprotonated Asp(2.50), where its disruption takes place while both Arg(3.50) and helix VI adopt a position similar to the one in the crystal structure of active opsin (Fig. 4).

To further explore whether the correlation between the protonation state of Asp(2.50) and ionic-lock conformation could be influenced by the ligand bound to the receptor (since both co-crystallized ligands show inverse agonist/antagonist activity), we performed additional simulations of unligated and agonist-bound β_2AR in both possible protonation states of Asp(2.50). All simulations yielded fully consistent results [i.e., ionic-lock formation is only induced when Asp(2.50) is protonated] (Fig. 3b).

According to a large number of biochemical studies suggesting that breaking of the salt bridge between Arg(3.50) and Glu(6.30) is an early key event in GPCR activation,[5,7,8] the equilibrium conformations we identified when Asp(2.50) is protonated are reminiscent of the inactive form of the receptors, while the conformation when Asp (2.50) is deprotonated retains typical structural characteristics of the active form.

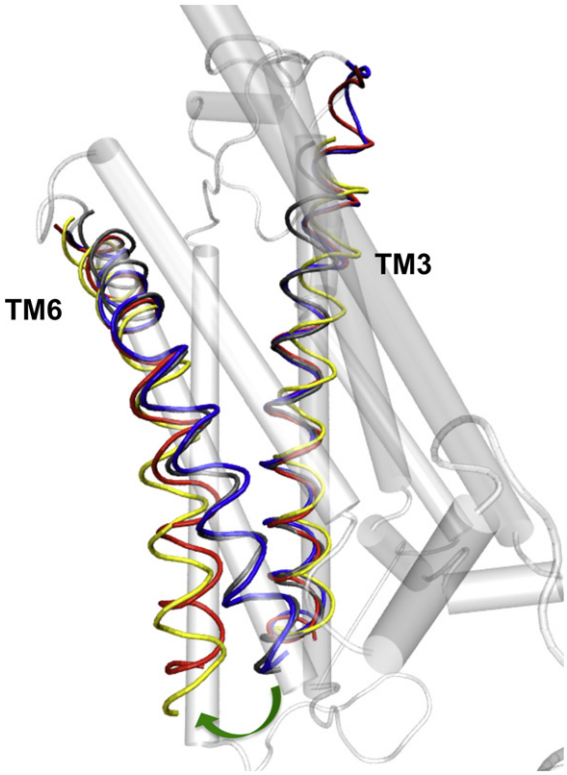

Fig. 4. Superposition of helices III and VI of crystal structures of dark rhodopsin (gray) and active opsin (yellow) and of equilibrated MD snapshots of cyanopindolol-bound wild-type β_1AR with a protonated Asp(2.50) (blue) and a deprotonated Asp(2.50) (red).

Signal transduction from Asp(2.50) to the cytoplasmatic side

The molecular details of GPCR signal transduction and the associated local conformational changes are still largely unclear. Several crucial residues have been identified on the basis of conservation analyses or mutagenesis experiments, and different activation mechanisms have been proposed.[5–7,10,15,16,23,24,40–42] However, due to the limited amount of structural data for diffusible ligand class A GPCRs, the precise role of these residues and the conformational transitions occurring inside the hydrophobic core of the receptor during the early steps of the activation process are yet to be determined. A comparison between the two conformations that we have identified permits to understand how a change in the protonation state of Asp(2.50) affects the equilibrium conformation of the cytoplasmatic end of the receptor and what local transitions are required to favor such an equilibrium shift.

Comparison between the computed contact maps of the simulations of the different protonation states (cf., Table S1) suggests that the polar residues connecting Asp(2.50) to the ionic-lock region (cf., Fig. 5) play a prominent role in signal transduction. Statistical analysis on the last 200 ns of simulations of wild-type receptors with their co-crystallized ligands indicates that while protonation of Asp (2.50) keeps a series of microswitches in a stable conformation, deprotonation of Asp(2.50) induces an increased instability that ultimately leads to ionic-lock opening via alteration of the electrostatic potential in the internal cavity of the receptor (Fig. 5).

This extended polar network reaches from Asp (2.50) to the ionic-lock via the highly conserved NPxxY motif and the polar pair Asn(2.40)Thr(2.39) that is located at the cytoplasmatic end of helix II, where the NPxxY motif acts as a hinge for the Asn (2.40)Thr(2.39) pair that undergoes a seesaw-like movement that ultimately leads to ionic-lock formation/breaking. In the inactive conformation, Asn

Fig. 3. (a) Time evolution of the C^{α}–C^{α} (red) distance and of the shortest N–O (blue) distance between Arg(3.50) and Glu(6.30) with Asp(2.50) deprotonated (upper panel) or protonated (lower panel). Averages are shown in corresponding continuous lines. The shadowed gray bar represents the corresponding C^{α}–C^{α} distance of crystal structures of dark-state rhodopsin; the green bar, set at 3.0 Å, indicates the distance corresponding to the formation of the ionic-lock salt bridge. (b) Time evolution of the C^{α}–C^{α} (red) distance and of the shortest N–O (blue) distance between Arg(3.50) and Glu(6.30) with Asp(2.50) deprotonated (upper panel) or protonated (lower panel) in β_2AR in its apo form (apo) or bound to the potent agonist isoprenaline (ISO). Averages are shown in corresponding continuous lines. The shadowed gray bar represents the corresponding C^{α}–C^{α} distance of crystal structures of dark-state rhodopsin; the green bar, set at 3.0 Å, indicates the distance corresponding to the formation of the ionic-lock salt bridge.

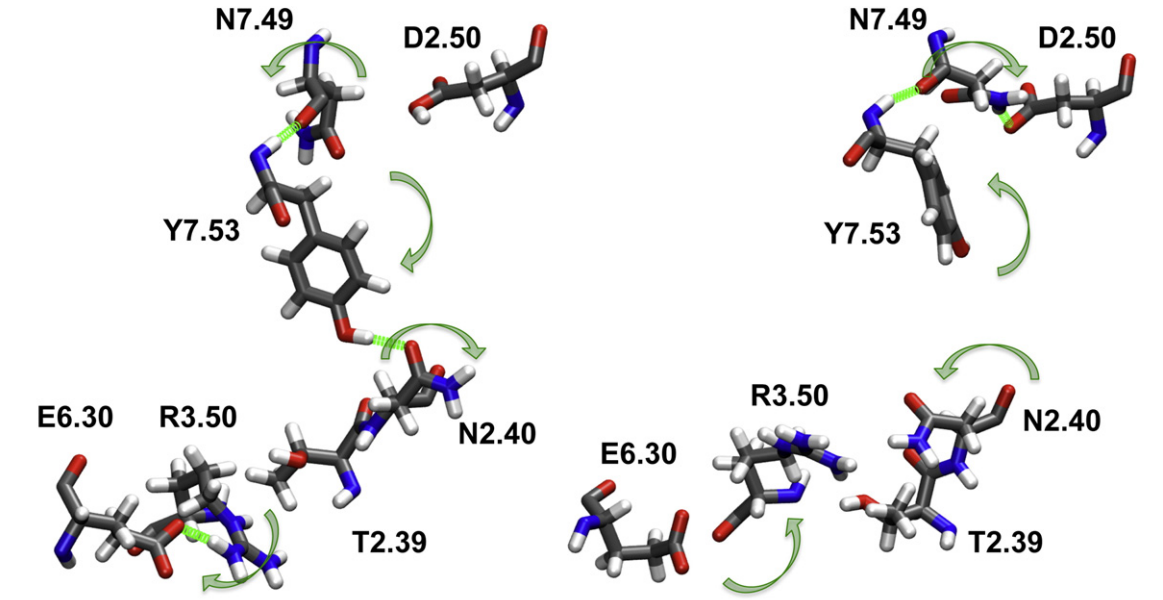

Asp2.50 protonated	β_1AR-wt	β_2AR-wt	Average value
D2.50-N7.49	1%	1%	1%
Y7.53-N2.40	58%	70%	70%
N2.40	98%	97%	97%
"ionic lock"	**99%**	**100%**	**100%**

Asp2.50 deprotonated	β_1AR-wt	β_2AR-wt	Average value
D2.50-N7.49	68%	99%	84%
Y7.53-N2.40	1%	63%	32%
N2.40	37%	0%	19%
"ionic lock"	**6%**	**1%**	**4%**

Fig. 5. Conformational transitions of internal microswitches connecting Asp(2.50) with the ionic lock. The upper panel shows snapshots of the interaction patterns of Asp(2.50), Asn(7.49), Tyr(7.53), Asn(2.40), Thr(2.39) and the ionic lock in simulations with Asp(2.50) protonated (left) and with Asp(2.50) deprotonated (right). The lower panel shows residence time, over the last 200 ns of each simulation, of the crucial interactions connecting Asp(2.50) to the ionic lock. D2.50–N7.49, N7.53–N2.40 and ionic lock (R3.50–E6.30) indicate the residence time of the contact between the two residues (with a cutoff of 2.2 Å), while N2.40 indicates the residence time of the χ_1 angle of Asn(2.40) in the *trans* conformation.

(7.49) of the NPxxY motif does not directly hydrogen-bond Asp(2.50), pointing toward the receptor core for 99% of the simulation time, while Tyr(7.53) of the NPxxY is strongly coupled to Asn(2.40), thus keeping helices II and VII close to each other (Fig. 5). This in turn keeps the χ_1 angle of Asn(2.40) permanently in the *trans* conformation, orienting the dipole arising from the side chain of the asparagine far away from the helix III–helix VI interface. As a consequence, also Thr(2.39) moves far apart from Arg(3.50), allowing Glu(6.30) to approach Arg(3.50) and to form the ionic-lock during the last 200 ns (Fig. 5). On the other hand, when Asp(2.50) is deprotonated, Asn(7.49) screens the negative charge via a hydrogen-bond interaction between its side chain and Asp(2.50). This in turn leads to a far greater instability of the helix II–helix VII interface, with Tyr (7.53) hydrogen-bonding Asn(2.40) only during very short time intervals, accounting for 32% of the simulation time. As a consequence, the χ_1 angle of Asn(2.40) tends to adopt the *gauche*(-) conformation, a configuration identical with the one present in the two available crystal structures of adrenergic receptors. In such a conformation, Thr(2.39) moves closer to Arg(3.50), forcing Glu(6.30) away from the arginine of the conserved DRY motif preventing ionic-lock formation (Fig. 5).

Discussion

The availability of GPCR crystal structures enables simulations of receptor structure and dynamics at the molecular level, paving the way for a deeper understanding of the activation mechanism upon ligand binding. Using MD simulations, we were able to elucidate the possible role of Asp(2.50) during receptor activation and allosteric regulation, identifying a direct correlation between the protonation state of this evolutionarily conserved residue and the ionic-lock conformation.

In the current paradigm of GPCR functioning, this interaction is formed in the inactive conformation of the receptors, while breakage of this interhelical salt bridge is associated to an outward movement of helix VI that enables recognition of the cognate G-protein via reorganization of the cytoplasmic side involving residues Asp(3.49), Arg(3.50), Tyr(5.58), Glu(6.30) and Tyr(7.53). Even if the current capabilities of MD simulations cannot deal with the timescales of the full activation cycle of GPCRs and despite the fact that many pathways might concur to activate the signaling cascade, we have been able to identify the effects of the protonation state of the highly conserved Asp(2.50) from the

local environment up to the cytoplasmic end that is involved in G-protein recognition.

In particular, in all simulations, protonation of Asp (2.50) leads to stable ionic-lock formation, indicating strong coupling between this conserved residue and the cytoplasmatic helix III–helix VI interface. Our findings are in agreement with several experiments showing that sodium acts as an allosteric inverse agonist via binding to Asp(2.50),[26,33,38,43] and they suggest a possible rationale for the altered constitutive and agonist-induced activity shown by site-directed substitution of D2.50 in adrenergic receptors and in other non-opsin class A GPCRs.[12–14,32,33,43]

The simulations also show that receptor inhibition upon charge neutralization in helix II is achieved via complex coupling between Asp(2.50) and the cytoplasmatic conformation of helices III and VI, leading to ionic-lock formation and to conformational changes in the most acknowledged interaction site between the receptor and its G-protein partner.

On the other hand, it is known that increasing the pH in the range between 6.5 and 8.0 leads to an increase of both agonist affinities and GTPase-mediated receptor saturation activity, while constitutive activity decreases.[44] This observation is not necessarily in contrast to our findings since this effect could originate from the involvement of other titrable residues in the activation mechanism, in particular Glu(3.49), which has been identified as the proton uptake site in the transition from MetaI to MetaII in rhodopsin. However, in the conceptual framework of GPCR activation, our simulations are consistent with the fact that acidification leads to reduced agonist-induced saturation activity, since a lowering of pH favors protonation of Asp(2.50), which in turn leads to ionic-lock formation[a].

Despite possible limitations occurring from the fact that the simulations have been performed on monomeric forms of the receptors and without the presence of the partner G-protein, our results suggest that while the global structural rearrangements of the transmembrane helices upon activation are similar in rhodopsin and adrenergic receptors, signal transduction upon ligand binding from the binding pocket to the cytoplasmic moiety seems to occur in a different way. While Asp(2.50) is only partially involved in rhodopsin activation, changing hydrogen-bond partners but keeping its neutral protonation state,[37] our findings show that in adrenergic receptors the protonation state of Asp (2.50) directly shifts the conformational equilibrium of the ionic-lock, suggesting that this conserved residue is probably charged in the active form of non-opsin class A GPCRs and that it can eventually undergo protonation change upon inhibition. Given its localization in the protein matrix, the simulations with a deprotonated Asp(2.50) suggest that internal water molecules directly connecting Asp(2.50) to the cytosol could mediate a possible protonation pathway or sodium ion access from the extracellular medium to the vicinity of the charged aspartic acid.

This difference between opsin and non-opsin class A GPCRs is a consequence of highly conserved amino acid substitutions around Asp(2.50) and of the different interactions arising in the binding pocket between the bound ligand and the receptor. Within this picture, electrostatic interactions and conformational changes occurring upon ligand binding in non-opsin GPCRs could alter the electrostatic potential and the pK_a of Asp(2.50), thus favoring one of the protonation states and, in turn, the active or the inactive form. Our findings help in elucidating the mechanism of signal transduction from Asp(2.50) to the G-protein interaction site, showing that a number of highly conserved residues cooperate to stabilize the receptor in its active/inactive conformation. In agreement with mutational studies[10] and with the available crystallographic structures, we observed that the interaction between helices II and VII, via Asp(2.50) and the highly conserved NPxxY motif, is crucial to determine the activation state of the receptor.

In addition, our simulations describe a direct correlation between the value of the χ_1 angle of Asn (2.40) and the ionic-lock conformation. This transition of the Asn(2.40) side chain significantly alters the electrostatic potential felt by Arg(3.50), thus explaining how highly conserved residues in helices II and VII, which are located far away from the G-protein interaction site, can ease the conformational transition of the receptor.

In summary, we have identified that the protonation state of the crucial residue Asp(2.50) directly influences the probability of ionic-lock formation via a series of conformational changes of highly conserved residues in helices II and VII, including the NPxxY motif and Asn(2.40). This mechanism, which is likely to be shared by most class A GPCRs, is not present in rhodopsin. Even though these are only preliminary steps toward a comprehension of the molecular details of GPCR function, we envision that emergence of new crystal structures together with computer simulations will be able to shed more light into the full activation process of such receptors that is of utmost pharmaceutical and biological relevance.

Materials and Methods

All simulations are based on the crystal structure of human β_2AR (PDB code 2RH1)[2] and on chain B of the

[a] Dror *et al.*, in their recent computational study,[20] reported microsecond MD simulations describing ionic-lock formation in multiple simulations for both Asp(2.50) protonation states. We identified the origin of this discrepancy in the different treatments of the electrostatic and van der Waals interactions. In fact, using the real space cutoff that Dror *et al.* used (which is below the usually recommended value[45]) within our setup (our force field, lipids and initial configuration), we can reproduce Dror *et al.*'s results, which show ionic-lock formation with a deprotonated Asp(2.50), while tests performed using a real space cutoff of 15 Å suggest that our simulations are converged with respect to the cutoff.

crystal structure of partially mutated (β_1AR-m23) turkey β_1AR (PDB code 2VT4) solved at 2.7-Å resolution.[3] MODELLER9v3[46–48] was used to add the missing amino acid residues 16–29 and 342–353 in the N-terminal and C-terminal tails of β_2AR, respectively, and residues 31–38 and 360–367 in the N-terminal and C-terminal tails of β_1AR, respectively. Amino acid residues 1–15 and 354–365 in β_2AR and residues 1–30 in β_1AR, which are also missing in the X-ray structure, were not included. The same software package has been used to model the third intracellular loop (residues 234–259 for β_2AR and residues 239–243 and 272–283 for β_1AR) choosing the loop with the lowest DOPE score.[49] The third intracellular loop of β_1AR was modeled maintaining the same deletion (residues 244–271) that was used to achieve crystallization. For wild-type β_1AR, residues S68, V90, A227, L282, A327 and M338 were mutated back to R68, M90, Y227, A282, F327 and F338.

In both receptors, all ionizable side chains and the C- and N-termini are in their default ionization states, except for Asp(2.50), which is modeled in both protonation states for all the systems, and for Glu(3.41), which is protonated in all simulations. All histidine residues present in the proteins are assumed to be protonated either in the N^{δ} position (His22, His269 and His296 for β_2AR; His180 for β_1AR) or in the N^{ε} position (His18, His93, His172, His178, His241 and His256 for β_2AR; His286 in β_1AR). Carazolol, cyanopindolol and isoprenaline carry a net positive charge of +1e.

Overall neutrality of the system at physiological ion concentration (100 mmol/l) was obtained adding 20 sodium and 30 chloride ions to the aqueous phase for β_2AR simulations with a protonated Asp(2.50), while 14 sodium and 30 chloride ions were added in the β_1AR system with a protonated Asp(2.50). A chloride ion was removed in the simulations with a deprotonated Asp (2.50). Heteroatoms (as defined in the PDB format) present in the crystal structures are not included in the model, except for internal water molecules, the ligands and a palmitic acid residue bound to Cys341 for β_2AR. The program Dowser[50] was used to locate internal cavities in the protein and to assess their hydrophilicity by means of calculating the interaction energy of a water molecule with the surrounding atoms. A water molecule was placed in a cavity if the interaction energy was stronger than −10 kcal/mol. By this criterion, which has been found to be able to distinguish well-hydrated from empty cavities,[50,51] 5 water molecules in addition to the ones resolved in the crystal structure were added for β_2AR, while in the case of β_1AR, 13 water molecules in addition to the seven crystallographic ones were added.

The lipid used for the membrane simulation is 1-stearoyl-2-oleoyl-*sn*-glycero-3-phosphoethanolamine. The length of the aliphatic tail was chosen in such a way as to optimize the hydrophobic matching between the protein and the lipid bilayer. The system was immersed in a box of water of approximately $90 \times 90 \times 105$ Å^3 containing 16,000 molecules. The box dimensions were chosen in such a way that the minimum distance between periodic images of the protein is always larger than 30 Å during the simulation. The protein was inserted into the membrane such that helix VIII lies at the hydrophobic–hydrophilic interface, with the hydrophilic residues pointing toward the aqueous phase. The total number of atoms in our models is about 90,000.

The all-atom AMBER/parm99SB[52] force field was used for the protein, carazolol, cyanopindolol and isoprenaline, whereas the AMBER/parm96 was used for the lipid bilayer in combination with the SPC[53] model for water. The force field for the palmitic acid from previous studies was used.[51] The atomic charges for carazolol, cyanopindolol and isoprenaline were derived by RESP[52,54,55] fitting using HF/6-31G* optimized structures, and electrostatic potentials were obtained using the Gaussian03 package.[56]

All data collections and equilibration runs were done using GROMACS 4.[57] Electrostatic interactions were calculated with the Ewald particle mesh method,[58] with a real space cutoff of 12 Å. Bonds involving hydrogen atoms were constrained using the LINCS[59] algorithm, and the time integration step was set to 2 fs. The system was coupled to a Nosé–Hoover thermostat[60,61] and to an isotropic Parrinello–Rahman barostat[62] at a temperature of 310 K and a pressure of 1 atm.

After insertion of the protein in a preequilibrated lipid bilayer, the system was minimized using steepest descent algorithm and then heated to 310 K in 1040 ps while keeping positional restraints on crystallographic C^{α} and ligand heavy atoms. The constraints were successively removed during three sets of 3-ns runs. Finally, the equilibration run was completed with a 6-ns run with positional restraints applied to the ligand heavy atoms.

Simulations of apo-form and isoprenaline-bound β_2AR were started from the equilibrated carazolol-bound structures after removal of the bound ligand or replacement of the bound carazolol with isoprenaline after superimposition of the N-C-C-OH motif shared by many adrenergic receptor agonists and antagonists.

All data analyses were done using GROMACS[57] utilities, and all molecular images were made with Visual Molecular Dynamics;[63] Poisson–Boltzmann pK_a calculations[64] in Table 1 were made using the H^{++} server[b].

Acknowledgements

This work was supported by the Swiss National Science Foundation through grant 200020-116294. We thank Pablo Campomanes for helpful discussions.

Supplementary Data

Supplementary data associated with this article can be found, in the online version, at doi:10.1016/j.jmb.2010.01.060

References

1. Lundstrom, K. (2006). Latest development in drug discovery on G protein-coupled receptors. *Curr. Protein Pept. Sci.* **7**, 465–470.
2. Cherezov, V., Rosenbaum, D. M., Hanson, M. A., Rasmussen, S. G., Thian, F. S., Choi, H. J. *et al.* (2007). High-resolution crystal structure of an engineered human beta2-adrenergic G protein-coupled receptor. *Science*, **318**, 1258–1265.
3. Warne, T., Serrano-Vega, M. J., Baker, J. G., Moukhametzianov, R., Edwards, P. C., Henderson, R. *et al.* (2008). Structure of a beta1-adrenergic G-protein-coupled receptor. *Nature*, **454**, 486–492.

[b] http://biophysics.cs.vt.edu/H++

4. Weis, W. I. & Kobilka, B. K. (2008). Structural insights into G-protein-coupled receptor activation. *Curr. Opin. Struct. Biol.* **18**, 734–740.
5. Ballesteros, J. A., Jensen, A. D., Liapakis, G., Rasmussen, S. G. F., Shi, L., Gether, U. & Javitch, J. A. (2001). Activation of the beta(2)-adrenergic receptor involves disruption of an ionic lock between the cytoplasmic ends of transmembrane segments 3 and 6. *J. Biol. Chem.* **276**, 29171–29177.
6. Lei, S., Liapakis, G., Xu, R., Guarnieri, F., Ballesteros, J. A. & Javitch, J. A. (2002). beta(2) adrenergic receptor activation—modulation of the proline kink in transmembrane 6 by a rotamer toggle switch. *J. Biol. Chem.* **277**, 40989–40996.
7. Shapiro, D. A., Kristiansen, K., Weiner, D. M., Kroeze, W. K. & Roth, B. L. (2002). Evidence for a model of agonist-induced activation of 5-hydroxytryptamine 2A serotonin receptors that involves the disruption of a strong ionic interaction between helices 3 and 6. *J. Biol. Chem.* **277**, 11441–11449.
8. Scheer, A., Costa, T., Fanelli, F., De Benedetti, P. G., Mhaouty-Kodja, S., Abuin, L. *et al.* (2000). Mutational analysis of the highly conserved arginine within the Glu/Asp-Arg-Tyr motif of the alfa1b-adrenergic receptor: effects on receptor isomerization and activation. *Mol. Pharmacol.* **57**, 219–231.
9. Barak, L. S., Menard, L., Ferguson, S. S. G., Colapietro, A. M. & Caron, M. G. (1995). The conserved seven-transmembrane sequence NP(X)2,3Y of the G-protein-coupled receptor superfamily regulates multiple properties of the beta(2)-adrenergic receptor. *Biochemistry*, **34**, 15407–15414.
10. Urizar, E., Claeysen, S., Deupi, X., Govaerts, C., Costagliola, S., Vassart, G. & Pardo, L. (2005). An activation switch in the rhodopsin family of G protein-coupled receptors. *J. Biol. Chem.* **280**, 17135–17141.
11. Vogel, R., Mahalingam, M., Ludeke, S., Huber, T., Siebert, F. & Sakmar, T. P. (2008). Functional role of the "ionic lock"—an interhelical hydrogen-bond network in family A heptahelical receptors. *J. Mol. Biol.* **380**, 648–655.
12. Proulx, C. D., Holleran, B. J., Boucard, A. A., Escher, E., Guillemette, G. & Leduc, R. (2008). Mutational analysis of the conserved $Asp^{2.50}$ and ERY motif reveals signaling bias of the urotensin II receptor. *Mol. Pharmacol.* **74**, 552–561.
13. Bihoreau, C., Monnot, C., Davies, E., Teutsch, B., Bernstein, K. E., Corvol, P. & Clauser, E. (1993). Mutation of Asp74 of the rat angiotensin II receptor confers changes in antagonist affinities and abolishes G-protein coupling. *Proc. Natl Acad. Sci. USA*, **90**, 5133–5137.
14. Baker, J. G., Proudman, R. G. W., Hawley, N. C., Fischer, P. M. & Hill, S. J. (2008). Role of key transmembrane residues in agonist and antagonist actions at the two conformations of the human beta (1)-adrenoceptor. *Mol. Pharmacol.* **74**, 1246–1260.
15. Greasley, P. J., Fanelli, F., Rossier, O., Abuin, L. & Cotecchia, S. (2002). Mutagenesis and modelling of the alpha(1b)-adrenergic receptor highlight the role of the helix 3/helix 6 interface in receptor activation. *Mol. Pharmacol.* **61**, 1025–1032.
16. Fritze, O., Filipek, S., Kuksa, V., Palczewski, K., Hofmann, K. P. & Ernst, O. P. (2003). Role of the conserved NPXXY(x)(5,6)F motif in the rhodopsin ground state and during activation. *Proc. Natl Acad. Sci. USA*, **100**, 2290–2295.
17. Palczewski, K., Kumasaka, T., Hori, T., Behnke, C. A., Motoshima, H., Fox, B. A. *et al.* (2000). Crystal structure of rhodopsin: a G protein-coupled receptor. *Science*, **289**, 739–745.
18. Okada, T., Sugihara, M., Bondar, A. N., Elstner, M., Entel, P. & Buss, V. (2004). The retinal conformation and its environment in rhodopsin in light of a new 2.2 Å crystal structure. *J. Mol. Biol.* **342**, 571–583.
19. Li, J., Edwards, P., Burghammer, M., Villa, C. & Schertler, G. F. X. (2004). Structure of a bovine rhodopsin in a trigonal crystal form. *J. Mol. Biol.* **343**, 1409–1438.
20. Dror, R. O., Arlow, D. H., Borhani, D. W., Jensen, M. O., Piana, S. & Shaw, D. E. (2009). Identification of two distinct inactive conformations of the beta2-adrenergic receptor reconciles structural and biochemical observations. *Proc. Natl Acad. Sci. USA*, **106**, 4689–4694.
21. Vanni, S., Neri, M., Tavernelli, I. & Rothlisberger, U. (2009). Observation of "ionic lock" formation in molecular dynamics simulations of wild-type beta1 and beta2 adrenergic receptors. *Biochemistry*, **48**, 4789–4797.
22. Park, J. H., Scheerer, P., Hofmann, K. P., Choe, H. W. & Ernst, O. P. (2008). Crystal structure of the ligand-free G-protein-coupled receptor opsin. *Nature*, **454**, 183–187.
23. Farrens, D. L., Altenbach, C., Yang, K., Hubbell, W. L. & Khorana, H. G. (1996). Requirement of rigid-body motion of transmembrane helices for light activation of rhodopsin. *Science*, **274**, 768–770.
24. Altenbach, C., Kusnetzow, A. K., Ernst, O. P., Hofmann, K. P. & Hubbell, W. L. (2008). High-resolution distance mapping in rhodopsin reveals the pattern of helix movement due to activation. *Proc. Natl Acad. Sci. USA*, **105**, 7439–7444.
25. Schwartz, T. W., Frimurer, T. M., Holst, B., Rosenkilde, M. M. & Elling, C. E. (2006). Molecular mechanism of 7TM receptor activation—a global toggle switch model. *Annu. Rev. Pharmacol.* **46**, 481–519.
26. Seifert, R. & Wenzel-Seifert, K. (2002). Constitutive activity of G-protein-coupled receptors: cause of disease and common property of wild-type receptors.. *Naunyn-Schmiedeberg's Arch. Pharmacol.* **366**, 381–416.
27. Vilardaga, J. P., Steinmeyer, G. S., Harms, G. S. & Lohse, M. J. (2005). Molecular basis of inverse agonism in a G protein-coupled receptor. *Nat. Chem. Biol.* **1**, 25–28.
28. Yao, X. J., Parnot, C., Deupi, X., Ratnala, V. R. P., Swaminath, G., Farrens, D. & Kobilka, B. (2006). Coupling ligand structure to specific conformational switches in the beta(2)-adrenoceptor. *Nat. Chem. Biol.* **2**, 417–422.
29. Zurn, A., Zabel, U., Vilardaga, J. P., Schindelin, H., Lohse, M. J. & Hoffmann, C. (2009). FRET-analysis of alpha2a-adrenergic receptor activation reveals distinct agonist-specific conformational changes. *Mol. Pharmacol.* **75**, 534–541.
30. Prioleau, C., Visiers, I., Ebersole, B. J., Weinstein, H. & Sealfon, S. C. (2002). Conserved helix 7 tyrosine acts as a multistate conformational switch in the 5HT2C receptor—identification of a novel "locked-on" phenotype and double revertant mutations. *J. Biol. Chem.* **277**, 36577–36584.
31. Pardo, L., Deupi, X., Doelker, N., Lopez-Rodriguez, M. L. & Campillo, M. (2007). The role of internal water molecules in the structure and function of the rhodopsin family of G protein-coupled receptors. *ChemBioChem*, **8**, 19–24.
32. Strader, C. D., Sigal, I. S., Candelore, M. R., Rands, E., Hill, W. S. & Dixon, A. F. (1988). Conserved aspartic

acid residues 79 and 113 of the beta-adrenergic receptor have different roles in receptor function. *J. Biol. Chem.* **263**, 10267–10271.
33. Ceresa, B. P. & Limbird, L. E. (1994). Mutation of an aspartate residue highly conserved among G-protein-coupled receptors results in nonreciprocal disruption of alpha2a-adrenergic receptor–G-protein interactions. *J. Biol. Chem.* **269**, 29557–29564.
34. Ahmed, M., Muntasir, H. A., Hossain, M., Ishiguro, M., Komiyama, T., Muramatsu, I. & Kurose, H. (2006). beta-Blockers show inverse agonism to a novel constitutively active mutant of beta(1)-adrenoceptor. *J. Pharmacol. Sci.* **102**, 167–172.
35. Weitz, C. J. & Nathans, J. (1993). Rhodopsin activation: effects on the metarhodopsin I–metarhodopsin II equilibrium of neutralization or introduction of charged amino acids within putative transmembrane segments. *Biochemistry*, **32**, 14176–141782.
36. Fahmy, K., Jager, F., Beck, M., Zvyaga, T. A., Sakmar, T. P. & Siebert, F. (1993). Protonation states of membrane-embedded carboxylic-acid groups in rhodopsin and metarhodopsin-II—a Fourier-transform infrared spectroscopy study of site-directed mutants. *Proc. Natl Acad. Sci. USA*, **90**, 10206–10210.
37. Rath, P., DeCaluwé, L. L. J., Bovee-Geurts, P. H. M., De Grip, W. J. & Rothschild, K. J. (1993). Fourier transform infrared difference spectroscopy of rhodopsin mutants: light activation of rhodopsin causes hydrogen-bonding change in residue aspartic acid-83 during meta II formation. *Biochemistry*, **32**, 10277–10282.
38. Parker, M. S., Wong, Y. Y. & Parker, S. L. (2008). An ion-responsive motif in the second transmembrane segment of rhodopsin-like receptors. *Amino Acids*, **35**, 1–15.
39. Man, O., Gilad, Y. & Lancet, D. (2004). Prediction of the odorant binding site of olfactory receptor proteins by human–mouse comparisons. *Protein Sci.* **13**, 240–254.
40. Azzi, M., Charest, P. G., Angers, S., Rousseau, G., Kohout, T., Bouvier, M. & Pineyro, G. (2003). beta-Arrestin-mediated activation of MAPK by inverse agonists reveals distinct active conformations for G protein-coupled receptors. *Proc. Natl Acad. Sci. USA*, **100**, 11406–11411.
41. Swaminath, G., Deupi, X., Lee, T. W., Zhu, W., Thian, F. S., Kobilka, T. S. & Kobilka, B. (2005). Probing the beta(2) adrenoceptor binding site with catechol reveals differences in binding and activation by agonists and partial agonists. *J. Biol. Chem.* **280**, 22165–22171.
42. Bhattacharya, S., Hall, S. E., Li, H. & Vaidehi, N. (2008). Ligand-stabilized conformational states of human beta(2) adrenergic receptor: insight into G-protein-coupled receptor activation. *Biophys. J.* **94**, 2027–2042.
43. Barbhaiya, H., McClain, R., Ijzerman, A. & Rivkees, S. A. (1996). Site-directed mutagenesis of the human A1 adenosine receptor: influences of acidic and hydroxy residues in the first four transmembrane domains on ligand binding. *Mol. Pharmacol.* **50**, 1635–1642.
44. Ghanouni, P., Schambye, H., Seifert, R., Lee, T. W., Rasmussen, S. G. F., Gether, U. & Kobilka, B. K. (2000). The effect of pH on beta2 adrenoceptor function. *J. Biol. Chem.* **275**, 3121–3127.
45. Brooks, B. R., Brooks, C. L., III, Mackerell, A. D., Nillson, L., Peterella, R. J., Roux, B. *et al.* (2009). CHARMM: the biomolecular simulation program. *J. Comput. Chem.* **30**, 1545–1615.
46. Fiser, A., Do, R. K. & Sali, A. (2000). Modeling of loops in protein structures. *Protein Sci.* **9**, 1753–1773.
47. Marti-Renom, M. A., Stuart, A. C., Fiser, A., Sanchez, R., Melo, F. & Sali, A. (2000). Comparative protein structure modeling of genes and genomes. *Annu. Rev. Biophys. Biomol. Struct.* **29**, 291–325.
48. Sali, A. & Blundell, T. L. (1993). Comparative protein modelling by satisfaction of spatial restraints. *J. Mol. Biol.* **234**, 779–815.
49. Shen, M. Y. & Sali, A. (2006). Statistical potential for assessment and prediction of protein structures. *Protein Sci.* **15**, 2507–2524.
50. Zhang, L. & Hermans, J. (1996). Hydrophilicity of cavities in proteins. *Proteins: Struct., Funct., Genet.* **24**, 433–438.
51. Rohrig, U., Guidoni, L. & Rothlisberger, U. (2002). Early steps of the intramolecular signal transduction in rhodopsin explored by molecular dynamics simulations. *Biochemistry*, **41**, 10799–10809.
52. Cornell, W. D., Cieplak, P., Bayly, C. I., Gould, I. R., Merz, K. M., Ferguson, D. M. *et al.* (1995). A 2nd generation force-field for the simulation of proteins, nucleic-acids, and organic-molecules. *J. Am. Chem. Soc.* **117**, 5179–5197.
53. Berendsen, H. J. C., Postma, J. P. M., Vangunsteren, W. F. & Hermans, J. (1981). Interaction models for water in relation to protein hydration. *Intermol. Forces*, 331–342.
54. Bayly, C. I., Cieplak, P., Cornell, W. D. & Kollman, P. A. (1993). A well-behaved electrostatic potential based method using charge restraints for deriving atomic charges—the RESP model. *J. Phys. Chem.* **97**, 10269–10280.
55. Wang, J. M., Cieplak, P. & Kollman, P. A. (2000). How well does a restrained electrostatic potential (RESP) model perform in calculating conformational energies of organic and biological molecules? *J. Comput. Chem.* **21**, 1049–1074.
56. Frisch, M. J., Trucks, G. W., Schlegel, H. B., Scuseria, G. E., Robb, M. A., Cheeseman, J. R. *et al.* (2004). Gaussian 03 Gaussian, Inc., Wallingford, CT.
57. Van der Spoel, D., Lindahl, E., Hess, B., Groenhof, G., Mark, A. E. & Berendsen, H. J. C. (2005). GROMACS: fast, flexible and free. *J. Comput. Chem.* **26**, 1701–1718.
58. Essmann, U., Perera, L., Berkowitz, M. L., Darden, T., Lee, H. & Pedersen, L. G. (1995). A smooth particle mesh Ewald method. *J. Chem. Phys.* **103**, 8577–8593.
59. Hess, B., Bekker, H., Berendsen, H. J. C. & Fraaije, J. G. E. M. (1997). LINCS: a linear constraint solver for molecular simulations. *J. Comput. Chem.* **18**, 1463–1472.
60. Nose, S. (1986). An extension of the canonical ensemble molecular-dynamics method. *Mol. Phys.* **57**, 187–191.
61. Hoover, W. G. (1985). Canonical dynamics—equilibrium phase–space distributions. *Phys. Rev. A*, **31**, 1695–1697.
62. Parrinello, M. & Rahman, A. (1981). Polymorphic transitions in single-crystals—a new molecular-dynamics method. *J. Appl. Phys.* **52**, 7182–7190.
63. Humphrey, W., Dalke, A. & Schulten, K. (1996). VMD—Visual Molecular Dynamics. *J. Mol. Graphics*, **14**, 33–38.
64. Yang, A. S., Gunner, M. R., Sampogna, R., Sharp, K. & Honig, B. (1993). On the calculation of p*K*(a)s in protein. *Proteins: Struct., Funct., Genet.* **15**, 252–265.
65. Bas, D. C., Rogers, D. M. & Jensen, J. H. (2008). Very fast prediction and rationalization of pK_a values for protein–ligand complexes. *Proteins: Struct., Funct., Genet.* **73**, 765–783.